energies

MDPI

Article

A Decoupled Design Parameter Analysis for Free-Piston Engine Generators

Boru Jia [1,2], Zhengxing Zuo [1], Andrew Smallbone [2,*], Huihua Feng [1] and Anthony Paul Roskilly [2]

1 School of Mechanical Engineering, Beijing Institute of Technology, Beijing 100081, China; boru.jia@newcastle.ac.uk (B.J.); zxzuo@bit.edu.cn (Z.Z.); fenghh@bit.edu.cn (H.F.)
2 Sir Joseph Swan Centre for Energy Research, Newcastle University, Newcastle upon Tyne NE1 7RU, UK; tony.roskilly@newcastle.ac.uk
* Correspondence: Andrew.Smallbone@newcastle.ac.uk; Tel.: +44-0191-208-4954

Academic Editor: Chang Sik Lee
Received: 16 February 2017; Accepted: 28 March 2017; Published: 4 April 2017

Abstract: The free-piston engine generator (FPEG) is a novel power generation device with an estimated brake efficiency (energy contained in the fuel that is transformed into useful work) of up to 46%, compared to the 25–35% reported in conventional reciprocating engines. This paper seeks to address a major challenge in the development of new and complex technologies—how do we effectively communicate and understand the influence of key design parameters on its operating performance? In this paper, the FPEG is described using a simple numerical model, a model which is reduced to a forced mass-spring vibration system under external excitation, enabling all the major input parameters to be decoupled. It proved that the engine piston position as a function of time and output power could be predicted directly from the input parameters with acceptable accuracy. The influence of the key FPEG design parameters on the piston oscillation characteristics and electric power output can be characterised with respect to one another and summarised. Key design parameters include piston mass, compression stroke length, piston cross sectional area, and electric load. Compared with previous and more complex numerical models, the presented methods can be used to simply describe the sensitivity of key design parameters on the FPEG performance. It will provide useful general guidance for the FPEG hardware design process.

Keywords: free-piston engine; generator; design parameters; numerical model; decoupled analysis

1. Introduction

1.1. Background

Free-piston engine (FPE) technology is currently being explored by a number of research groups worldwide, including the authors' group [1–8]. A significant driving force is the automotive industry's increasing investment in hybrid-electric vehicle technology. Known FPE applications include air compressors, hydraulic pumps, and electric generators [9]. In this paper, the FPE coupled with a linear electric generator (free-piston engine generator [FPEG]) is investigated with the objective to utilisation within a hybrid-electric vehicle. For the dual piston type FPEG, combustion in the chambers of the FPE occurs alternatively, which makes the translator move back and forth in a periodic way. The linear electrical machine located in the middle of the two cylinders converts parts of the mover's mechanical energy into electrical energy, which will be stored and/or used to power an external load. The estimated thermal efficiency (percentage of energy contained in the fuel that is transformed into useful work) is up to 46%, compared to the 25–35% reported in conventional reciprocating engines [10]. It shows promising results in terms of engine efficiency and exhaust gas emissions [10].

1.2. Literature Review

Unlike a reciprocating engine, the piston movement of the FPEG is not restricted by the crankshaft mechanism; the piston is instead only influenced by the gas (compression and expansion) and load forces acting upon it. As a result, the FPEG has specific and unique operation characteristics. To date, the free-piston engine has been most commonly modelled using simplified zero-dimensional (0D) methods [5,8,11–16]. In this section, the modelling and parametric study of the FPEG based on the available literature are summarised.

Atkinson et al., based in West Virginia University (WVU), developed an engine simulation model with the combination of piston dynamic and in-cylinder gas thermodynamic analyses [17–22]. To ensure the numerical model usefulness, the parameters used were based on experimental data obtained from an operating prototype, including piston position, piston velocity, and cylinder pressure. A parametric study was undertaken to evaluate the system operation characteristics. It was observed that, when the engine was operated at the same load, the peak in-cylinder pressure could be increased by decreasing the combustion duration. However, the influence on the overall useful work (via analysis of the pressure-volume diagram) was not that significant. The engine speed (or the operating frequency) proved to be higher with higher peak in-cylinder pressure. Also, a longer piston stroke length or higher compression ratio was also found with higher peak in-cylinder pressure [22].

Mikalsen and Roskilly from Newcastle University proposed an alternative FPEG design. The configuration consisted of a combustion chamber, a gas spring rebound device and a linear electric generator [12,23]. The sub-models for their modelling of the in-cylinder thermodynamics were based on the widely used thermodynamic models for the simulation of conventional reciprocating diesel engines. Results showed that the numerical model was able to predict the real trends of the designed FPE engine with various operation conditions [12]. It was apparent that the piston spent less time around the top dead centre (TDC) for the FPEG, where the cylinder gas pressure and temperature were the highest. Lower peak piston velocity was found for the FPEG, and very high acceleration was observed after ignition for the FPEG when the cylinder pressure was high and the piston was not restricted by the crankshaft mechanism in conventional engines. Simulated peak acceleration of the FPEG was reported to be around 60% higher than that of the conventional engine [12].

Goldsborough et al. at Sandia National Laboratories (SNL) analysed the operating characteristics of the designed FPEG during the stable operation state after successful engine cold start-up process [15,24–26]. A zero-dimensional thermodynamic numerical model was developed with detailed chemical kinetics for the heat release process, heat transfer, empirical scavenging, and frictional force sub models. Hydrogen was selected as the fuel for the designed FPEG system, and the simulation results indicated the key factors affecting the engine operation performance [15]. Their investigation on gas thermodynamics was based on a zero-dimensional approach, and the spatial effects and fluid dynamic were not taken into consideration. It was evident that the piston spent less time at TDC, and accelerated/decelerated faster at the end of the stroke. The corresponding characteristic of shorter time at TDC for the FPEG could be attractive on NO_x formation and heat transfer losses, since less residence times at higher temperatures were noted [15].

Researchers at Beijing Institute of Technology (BIT) presented simulation investigation on piston movement, using a simulation program developed in Matlab to define the piston's movement profiles [4,27,28]. They developed a detailed model for a U-shaped, three-phase linear electric generator with permanent magnets. The total electromagnetic resistance force produced by the linear generator during the generating process was derived [28]. Moreover, a multi-dimensional investigation on gas flows during the scavenging process of the FPEG was undertaken, based on the numerical simulation results. A wide range of design parameters and operating conditions were investigated to find out their influence on the scavenging performance, which included the effective stroke length, intake/exhaust valve overlapping, engine speed, and the intake charging pressure. The pressure in the cylinder and pressure in the scavenging pump were collected from a running prototype, and used to define the system boundary conditions [27].

Ocktaeck Lim et al., from University of Ulsan, presented an experimental and simulation study of a FPEG, which consisted of a two-stroke FPE, linear generators, and compressors [29]. Propane was used as fuel, and was premixed with the air to make a homogeneous charge. In the experimental study, the effects of input caloric value, equivalent ratio, spark timing delay etc., were investigated. The influence of the reciprocating mass, spark timing and spring stiffness on the piston dynamics and electric power output were studied. In addition, the highest generating power of the linear engine could be easily achieved by optimizing the key operation parameters [29].

1.3. Aims and Methodologies

In the development of new FPEG designs, the first stage is to size the system components and layout, based around meeting target operational characteristics. In a FPEG context, this is a major challenge, as there is very little data and only a handful of designs have ever operated and have been reported in the public domain. Furthermore, the studies outlined above only evaluated one design each and measured performance with respect to any system control parameters. In going beyond these works to produce a more holistic understanding of FPEG design and its impact on performance, it is only practical to use a modelling approach.

For reciprocating engines, answers for simple design questions, such as "What speed range will the engine operate at?", "How much power will this configuration generate?", "How does increasing the bore size affect the performance?" etc., have been known for a century with supporting models, data, and experience. However, this knowledge is not available for FPEG designs. This paper aims to fill this gap and present a decoupled analysis of a FPEG design to answer these kinds of questions, a solution which is underpinned by a validated fast-response numerical model. The dynamic characteristics of a dual-piston FPEG will be described, and the piston dynamics and output power can be predicted directly from the input parameters with acceptable accuracy. Unlike the above methods, the coupled differential equations do not need to be solved. Compared with the previous detailed numerical model with differential equations, the presented methods are simple and all the input parameters are decoupled. It will provide support for engineers and scientists engaged in the first stage of the FPEG hardware design process.

2. Design Parameters Analysis

2.1. FPEG Configuration

The FPEG configuration and prototype are shown in Figure 1a,b respectively. The main parts of the FPEG system consist of two internal combustion engines and a linear electric machine. The linear mover with pistons at each end is located between the two internal combustion engines, which forms the only significant moving part of the system. The engine employs a two-stroke gas exchange process, and the power stroke is controlled to take place alternatingly in each cylinder to overcome the compression force in the opposite cylinder. The scavenging ports are covered and uncovered by the piston, and the opening area is determined by the piston movement. As a result, the mover coupled with two pistons reciprocates between its two dead centres, and the linear electric generator converts this mechanical energy into electrical energy. More details on the prototype and its development approach can be found in our previous publications [3,5,30–32].

When the engine is successfully initialised by the linear electric machine with a mechanical resonance method [3,5,31], the fuel delivery and ignition systems are activated and the electrical discharge between the spark plug electrodes starts the heat release process at the end of the compression stroke [30]. The prototype specifications and the values of the main input parameters are listed in Table 1.

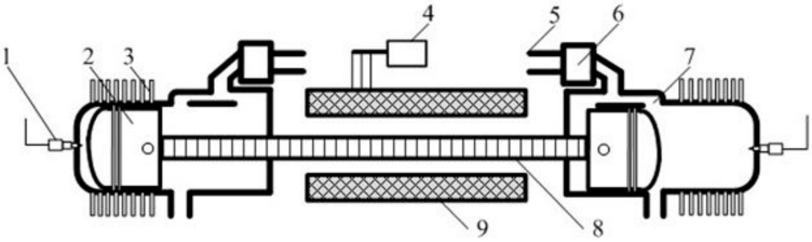

1 Spark plug; 2 Piston; 3 Cooling fin; 4 Load; 5 Air intake; 6 Fuel supply system;
7 Scavenging port; 8 Mover; 9 Stator

(**a**)

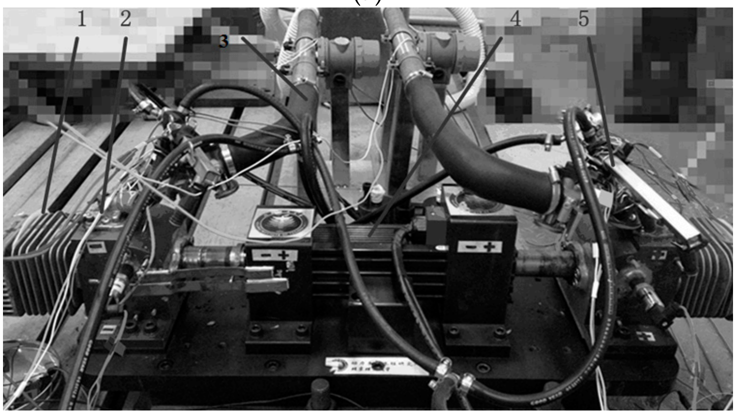

1 Cylinder; 2 Scavenging pump; 3 Air intake manifold;
4 Linear electric machine; 5 Fuel injection system

(**b**)

Figure 1. Free-piston engine generator (FPEG) configuration and prototype [31]. (**a**) FPEG configuration; (**b**) FPEG prototype.

Table 1. Prototype specifications.

Parameters	Value
Maximum total stroke length [mm]	70.0
Compression stroke length [mm]	35.0
Ignition position from middle stroke [mm]	30.0
Bore size [mm]	52.5
Moving mass [kg]	5.0
Coefficient of the load force [N/(m·s^{-1})]	395.0
Ambient temperature [°C]	25.0

2.2. Fast Response Numerical Model

For the dual-piston FPE configuration, the engine is operated using a two-stroke gas exchange cycle, and combustion takes place alternatingly in each cylinder during stable generating. As there is compressible gas in the cylinders, this is considered to act like nonlinear springs. As such, here the FPEG system is considered to be analogous to a mass-spring vibration system under external excitation determined by the heat released during the combustion process [33]. The analogies between a mass-spring-damper and a FPEG system are summarised in Table 2.

Table 2. Analogy between a mass-spring-damper and a FPEG system [34].

Mass-Spring-Damper	FPEG System
Moving mass, m	Mass of piston assembly and mover, m
Damping coefficient, c	Linear generator load force, $c = k_v$
Spring constant, k	In-cylinder pressure, $k = \frac{2\gamma p_0 A}{L_s} + \frac{m_f H_u R \gamma}{C_v {L_s}^2 CR^{\gamma-1}}$
Excitation force, $F(t)$	Force from heat release/combustion, $F(t) = F_0 \sin \omega t$, $F_0 = \frac{4}{\pi} \frac{m_f H_u R}{CR^{\gamma-1} L_s C_v}$

In Table 2, k_v means the coefficient of the load force; γ is the heat capacity ratio; p_0 is the ambient pressure; A is the piston area; L_s is the half stroke length; m_f is the injected fuel mass per cycle for each cylinder; H_u is the heating value of the fuel; R is the gas constant; C_v is the heat capacity at constant volume; CR is the set compression ratio; F_0 is the amplitude of the excitation force; ω is the angular natural frequency.

Assumptions are made to simplify and linearize the FPEG system, i.e., (a) energy consumed by the gas leakage through the piston rings and heat transfer to the cylinder walls are not taken into consideration; (b) the running cycle is two adiabatic compression/expansion processes caused by engine volume change connected with a constant volume combustion process. The expected geometric compression ratio of the free-piston engine CR is affected by the ignition timing.

The FPEG system is finally simplified to a forced mass-spring vibration system under external excitation. Details for the model simplification and linearization can be found in [34]. The simplified dynamic equation is finally described as below:

$$m\ddot{x} + c\dot{x} + kx = F(t), \tag{1}$$

where m is the moving mass, which is 5.0 kg; c is the damping coefficient, which is 395.0; k is the spring constant with an estimated value of 6×10^4.

The solution for the piston displacement, x can be obtained according to vibration theory [35], and it is defined by:

$$x = -\frac{F_0 \cos \omega_n t}{c\omega_n}, \tag{2}$$

where the amplitude of the excitation force, F_0 and the damping coefficient, c can be obtained from Table 2, and the angular natural frequency, ω_n of the FPEG system is expressed as:

$$\omega_n = \sqrt{\frac{k}{m}}, \tag{3}$$

2.3. Model Validation Results

The solution for the piston displacement was calculated in Matlab/Simulink, using parameters obtained from the operating FPEG prototype shown in Figure 1. Wide throttle opening was applied with stoichiometric air-fuel ratio. The data in Figure 2 shows the simulated piston displacement compared with the experimental data at the same operating condition. The piston dynamics predicted from the numerical model show similar trends with the test data, and the observed amplitudes are almost identical. The observed difference can be controlled in less than 3%, which is considered acceptable due to the simplifications and assumptions applied when linearizing the model. Thus, the model is considered of sufficient robustness to evaluate the actual FPEG system performance. More validation results can be found in [34].

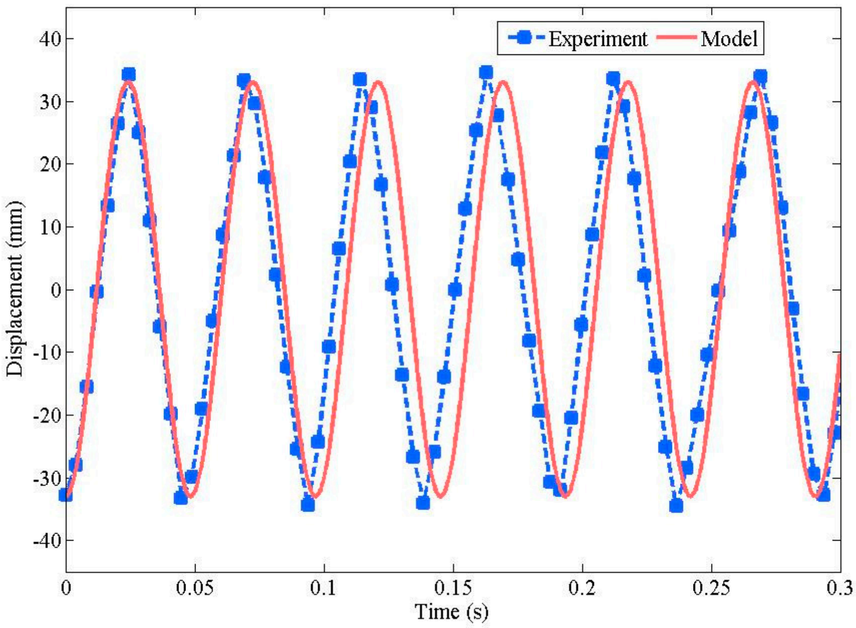

Figure 2. Model validation results.

2.4. Sensitivity Analysis of Design Parameters

When the viscous damped, the single degree-of-freedom FPEG system shown in Table 2 undergoes vibration defined by Equation (2); the velocity of the oscillation system, v (m/s) can be calculated by:

$$v = \dot{x}, \tag{4}$$

$$\dot{x} = \frac{F_0 \sin \omega_n t}{c}, \tag{5}$$

Also, the acceleration of the moving mass, a (m^2/s), can be expressed as:

$$a = \ddot{x}, \tag{6}$$

$$\ddot{x} = \frac{F_0 \omega_n \cos \omega_n t}{c}, \tag{7}$$

The amplitudes of the displacement, velocity, and acceleration of the moving mass are listed below:

$$|x| = \frac{F_0}{c\omega_n}, \tag{8}$$

$$|v| = \frac{F_0}{c}, \tag{9}$$

$$|a| = \frac{F_0 \omega_n}{c}, \tag{10}$$

Substituting F_0, c, and ω_n from previous equations, the Equations (8)–(10) can be rewritten as:

$$|x| = \frac{4K_t \cdot H_u}{\pi k_v C_v T_0 \text{ AFR } \text{CR}^{\gamma-1}\sqrt{2\gamma + \frac{K_t H_u \gamma}{C_v T_0 \text{AFR } \text{CR}^{\gamma-1}}}} \cdot \sqrt{A p_0 m L_s}, \tag{11}$$

$$|v| = \frac{4K_t H_u p_0}{\pi k_v C_v T_0 \text{ AFR CR}^{\gamma-1}} \cdot A, \tag{12}$$

$$|a| = \frac{4K_t H_u \sqrt{2\gamma + \dfrac{K_t H_u \gamma}{C_v T_0 \text{AFR CR}^{\gamma-1}}}}{\pi k_v C_v T_0 \text{ AFR CR}^{\gamma-1}} \cdot A p_0 \sqrt{\frac{p_0 A}{m L_s}}, \tag{13}$$

The natural frequency, F_n, of the FPEG is defined below, and it can be improved by reducing the moving mass or by increasing the bore/stroke ratio.

$$F_n = \frac{\omega_n}{2\pi} = \frac{1}{2\pi} \sqrt{2\gamma + \frac{K_t H_u \gamma}{C_v T_0 \text{AFR CR}^{\gamma-1}}} \cdot \sqrt{\frac{p_0 A}{m L_s}}, \tag{14}$$

The electric load force is known to have high effect on the operation characteristics of the FPEG system. According to reported literatures, the load force is a function of the design parameters of the linear electric generator, the mover's velocity, as well as the resistance of the external load [12–14]. The direction of the load force is always opposite to the direction of piston velocity, which acts as a resistance force. It is assumed to be proportional to the mover's speed, detailed description and model development process can be found in [13]. The force from the linear electric generator is described as below:

$$F_e = -k_v \dot{x} = -c\dot{x}, \tag{15}$$

where k_v is the constant of electric load ($\text{N}/(\text{m}\cdot\text{s}^{-1})$), which can be obtained from the linear electric generator design specifications, and the resistance of the external load. In general, higher k_v means a larger size of the linear electric generator.

Then, the output electric power from the linear generator, P_e, can be calculated from the electric load force:

$$P_e = \frac{F_0^2}{2c} = \frac{8}{k_v} \left(\frac{K_t H_u p_0}{\pi C_v T_0 \text{ AFR CR}^{\gamma-1}} \right)^2 \cdot A^2, \tag{16}$$

Compared with the commonly used detailed numerical model [13], the presented fast-response model is simplified and all the input parameters are decoupled. The piston dynamics and output electric power can be predicted directly from the input parameters with acceptable accuracy, without solving the coupled differential equations. From Equation (11) to Equation (16), the influence of the design parameters (m, L, A, and k_v) on the system oscillation characteristics and power output is shown in Table 3. It will provide useful general guidance for the design process, as well as accurate prediction for the future control of piston dynamics.

Table 3. Sensitivity analysis results of design parameters.

Design Target	Model Description	Design Parameter	Influence
Piston amplitude, $\lvert x \rvert$ [m]	$\lvert x \rvert = \frac{4K_t \cdot H_u}{\pi k_v C_v T_0 \text{ AFR CR}^{\gamma-1}\sqrt{2\gamma + \frac{K_t H_u \gamma}{C_v T_0 \text{AFR CR}^{\gamma-1}}}} \cdot \sqrt{A p_0 m L_s}$	Piston area, A [m]	$\lvert x \rvert \propto \sqrt{A}$
		Moving mass, m [kg]	$\lvert x \rvert \propto \sqrt{m}$
		Compression stroke, L_s [m]	$\lvert x \rvert \propto \sqrt{L_s}$
		Coefficient of electric load force [N/(m·s^{-1})]	$\lvert x \rvert \propto \frac{1}{k_v}$
Peak piston velocity, $\lvert v \rvert$ [m/s]	$\lvert v \rvert = \frac{4K_t H_u p_0}{\pi k_v C_v T_0 \text{ AFR CR}^{\gamma-1}} \cdot A$	Piston area, A [m]	$\lvert v \rvert \propto A$
		Coefficient of electric load force [N/(m·s^{-1})]	$\lvert v \rvert \propto \frac{1}{k_v}$
Peak piston acceleration, $\lvert a \rvert$ [m/s^2]	$\lvert a \rvert = \frac{4K_t H_u \sqrt{2\gamma + \frac{K_t H_u \gamma}{C_v T_0 \text{AFR CR}^{\gamma-1}}}}{\pi k_v C_v T_0 \text{ AFR CR}^{\gamma-1}} \cdot A p_0 \sqrt{\frac{p_0 A}{m L_s}}$	Piston area, A [m]	$\lvert a \rvert \propto A\sqrt{A}$
		Moving mass, m [kg]	$\lvert a \rvert \propto \frac{1}{\sqrt{m}}$
		Compression stroke, L_s [m]	$\lvert a \rvert \propto \frac{1}{\sqrt{L_s}}$
		Coefficient of electric load force [N/(m·s^{-1})]	$\lvert a \rvert \propto \frac{1}{k_v}$
Frequency, F_n [Hz]	$F_n = \frac{\omega_n}{2\pi} = \frac{1}{2\pi}\sqrt{2\gamma + \frac{K_t H_u \gamma}{C_v T_0 \text{AFR CR}^{\gamma-1}}} \cdot \sqrt{\frac{p_0 A}{m L_s}}$	Piston area, A [m]	$\lvert F_n \rvert \propto \sqrt{A}$
		Moving mass, m [kg]	$\lvert F_n \rvert \propto \frac{1}{\sqrt{m}}$
		Compression stroke, L_s [m]	$\lvert F_n \rvert \propto \frac{1}{\sqrt{L_s}}$
Electric power output, P_e [W]	$P_e = \frac{8}{k_v}\left(\frac{K_t H_u p_0}{\pi C_v T_0 \text{ AFR CR}^{\gamma-1}}\right)^2 \cdot A^2$	Piston area, A [m]	$P_e \propto A^2$
		Coefficient of electric load force [N/(m·s^{-1})]	$P_e \propto \frac{1}{k_v}$

3. Simulation Results and Discussion

When the design parameters change from a wide range from −50% to 50%, compared with the reference value listed in Table 1, i.e., without considering its physical feasibility, the influence on the design target is simulated. During the simulation, the engine was assumed to be operated at stoichiometric air-fuel ratio, and a wide open throttle (WOT) was applied. Other operational parameters in the model remain unchanged throughout the simulation.

The data in Figure 3 presents how the design parameters affect the piston amplitude. The influence of the piston cross-sectional area, moving mass, and the compression stroke length on the piston amplitude are identical, generally linear, and monotonic. Any change on these design parameters will lead to charge changes in piston TDC and compression ratio (CR). For the prototype with an engine effective stroke length of 35 mm, as adopted in this research, a TDC variation of ±1% of the stroke length would be equivalent to 0.35 mm and would produce a CR variation of approximately ±1.0.

The electric load plays a very important role during the matching design process and, in principle, can be changed in real-time during operation. From Figure 3, it is observed that the electric load is a more effective parameter for increasing the piston amplitude, and the piston amplitude or piston TDC will be improved significantly by reducing the electric load.

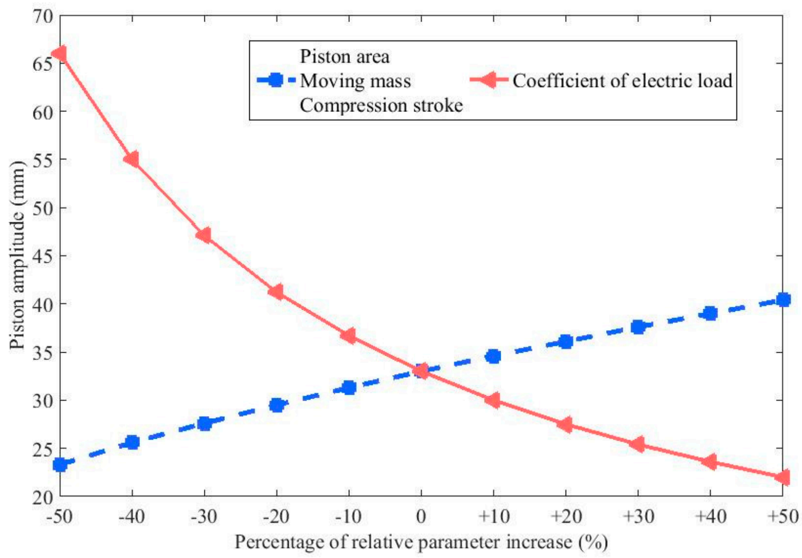

Figure 3. Influence of design parameters on piston amplitude.

Shown in Figure 4, the piston peak velocity is only affected by the piston cross sectional area and the electric load. The peak piston velocity is generally proportional to the piston area. If the peak velocity is expected to be over 10 m/s, with fixed electric load, the piston area is then suggested to increase 150% from its reference value. The electric load was found to be more effective in increasing the peak piston velocity, and the peak velocity can be increased obviously by decreasing the electric load. However, if a lower peak velocity is expected, then the piston area proves more influential.

Illustrated in Figure 5, all the design parameters—piston area, moving mass, compression stroke, and electric load—are shown to influence the peak piston acceleration. The peak acceleration can be increased by decreasing the moving mass/compression stroke/electric load, or enlarging the corresponding piston cross-sectional area. The changing trend of the electric load is similar with that of the moving mass and the compression stroke, while the peak acceleration is more sensitive to the electric load. If a lower peak acceleration is required (lower than approximately 450 m/s^2 for example), then the piston area is suggested to be used as it is the most effective design parameter to achieve this, and the peak acceleration can be reduced by decreasing the piston area.

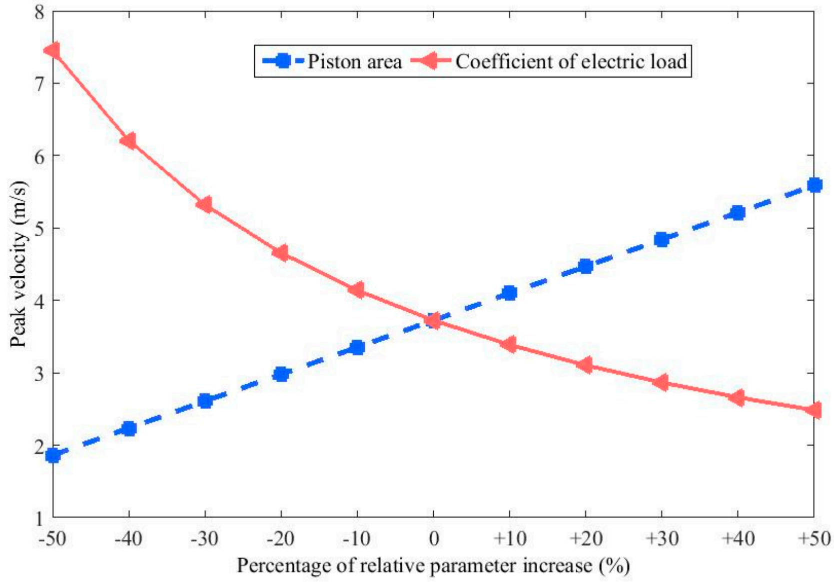

Figure 4. Influence of design parameters on piston peak velocity.

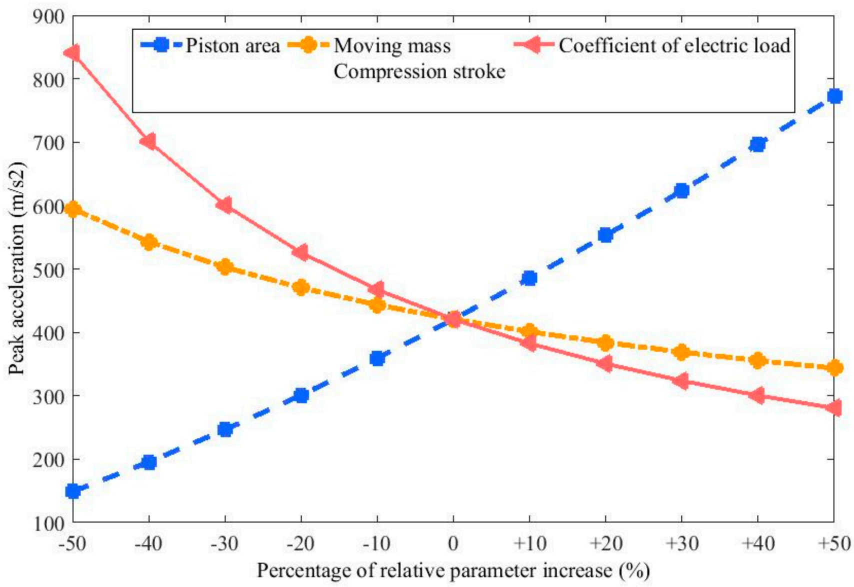

Figure 5. Influence of design parameters on piston peak acceleration.

The engine frequency can be influenced by the piston area, moving mass, and compression stroke length, as shown in Figure 6. The frequency could be increased by decreasing the moving mass/compression stroke, or enlarging the piston area. If the engine is expected to operate at a higher frequency (higher than 20 Hz), then the moving mass and the compression stroke length are proving more effective than the piston area; while, if a lower engine frequency is expected (lower than 20 Hz), the piston area is suggested to be adjusted. However, by changing these parameters by −50% to 50% from the reference values, the engine frequency is limited to 28 Hz (equivalent to 1680 rpm). As a result, for a FPEG of comparable size with the one used here, the engine is prone to operate at a low speed compared with the conventional reciprocating engines.

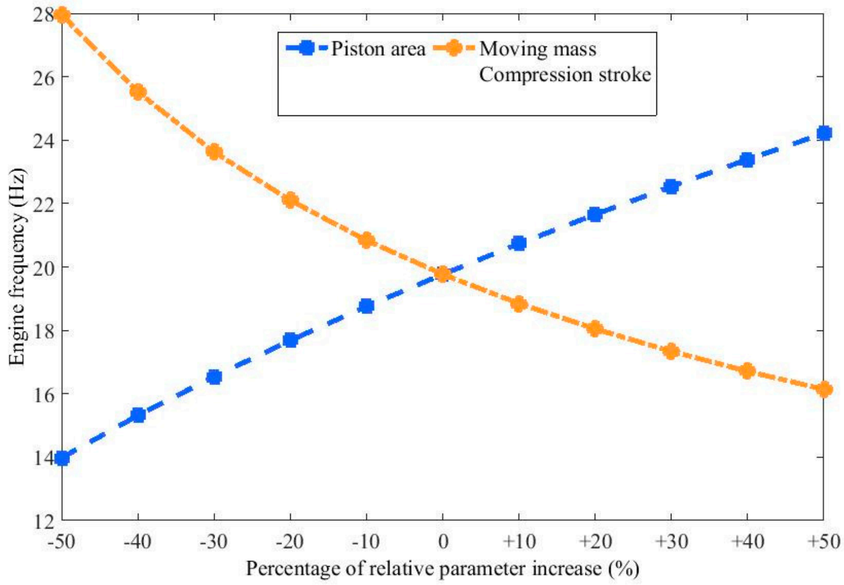

Figure 6. Influence of design parameters on engine frequency.

The data presented in Figure 7 demonstrates that the electric output power is only influenced by the piston area and the electric load, and the piston area is found to be more important for the power output. By enlarging the piston area, the engine swept volume (or capacity) is also increased. If a stoichiometric air-fuel ratio is adopted, then more fuel will be burnt and more power will be generated. However, for a FPEG system of comparable size with the one adopted here, the output electric power is limited to approximately 6 kW. If the energy demand is higher than that, then a larger engine bore or a lower electric load would be expected.

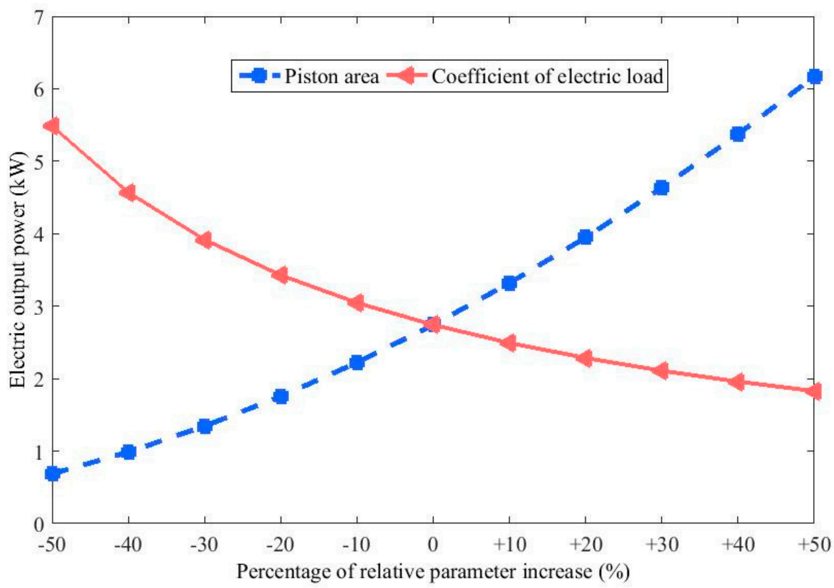

Figure 7. Influence of design parameters on electric power output.

4. Conclusions

In this paper, the FPEG system was described by a forced mass-spring vibration system under external excitation, and all the input parameters were decoupled. The piston dynamics and output power could be predicted directly from the input parameters with acceptable accuracy. The influence of the design parameters—i.e., piston mass, compression stroke length, piston area, and electric load—on the piston oscillation characteristics and electric power output were summarised. Compared with the previous complex numerical model, the presented methods are simple and all of the input parameters are decoupled. It will provide useful general guidance for the FPEG hardware design process. The main conclusions are listed below:

(1) the influence of the piston area, moving mass, and the compression stroke length on the piston amplitude is identical;
(2) the piston peak velocity is only affected by the piston area and the electric load;
(3) All of the design parameters—i.e., piston area, moving mass, compression stroke, and electric load—are effective to the peak piston acceleration;
(4) the electric output power is only influenced by the piston area and the electric load.

However, for a FPEG system of comparable size with the one adopted here, the output electric power is limited to approximately 6 kW.

Acknowledgments: This work was funded using the EPSRC (Engineering and Physical Sciences Research Council) Impact Acceleration Account EP/K503885/1 and National Nature Science Foundation of China (51006010). Data supporting this publication is openly available under an Open Data Commons Open Database License. Additional metadata are available at: http://dx.doi.org/. Please contact Newcastle Research Data Service at rdm@ncl.ac.uk for access instructions.

Author Contributions: Boru Jia completed the simulation and wrote the manuscript. Zhengxing Zuo and Huihua Feng conducted the experimental measurement and related data analysis. Andrew Smallbone and Anthony Paul Roskilly contributed the method and revised the manuscript.

Conflicts of Interest: The authors declare no conflict of interest.

Nomenclature

A	piston area
AFR	air-fuel ratio
B	cylinder bore
c	damping coefficient
C_v	heat capacity at constant volume
CR	set compression ratio
F	excitation force
F_0	amplitude of excitation force
F_e	resistant force from generator
k	spring constant or stiffness
k_v	coefficient of the load force
K_t	throttle opening coefficient
L_s	half stroke length
m	moving mass
m_f	fuel mass in the mixture
p	cylinder gas pressure
p_0	ambient pressure
Q_LHV	lower heating value
V	cylinder volume
V_o	cylinder volume at the middle stroke
x	mover displacement
ω_n	angular natural frequency
η_c	combustion efficiency

References

1. Chiang, C.J.; Yang, J.L.; Lan, S.Y.; Shei, T.W.; Chiang, W.S.; Chen, B.L. Dynamic modeling of a SI/HCCI free-piston engine generator with electric mechanical valves. *Appl. Energy* **2013**, *102*, 336–346. [CrossRef]

2. Hanipah, M.R.; Mikalsen, R.; Roskilly, A.P. Recent commercial free-piston engine developments for automotive applications. *Appl. Therm. Eng.* **2015**, *75*, 493–503. [CrossRef]
3. Jia, B.; Zuo, Z.; Feng, H.; Tian, G.; Roskilly, A.P. Investigation of the starting process of free-piston engine generator by mechanical resonance. *Energy Procedia* **2014**, *61*, 572–577. [CrossRef]
4. Feng, H.; Song, Y.; Zuo, Z.; Shang, J.; Wang, Y.; Roskilly, A.P. Stable Operation and Electricity Generating Characteristics of a Single-Cylinder Free Piston Engine Linear Generator: Simulation and Experiments. *Energies* **2015**, *8*, 765–785. [CrossRef]
5. Jia, B.; Zuo, Z.; Feng, H.; Tian, G.; Smallbone, A.; Roskilly, A.P. Effect of closed-loop controlled resonance based mechanism to start free piston engine generator: Simulation and test results. *Appl. Energy* **2016**, *164*, 532–539. [CrossRef]
6. Feng, H.; Guo, C.; Yuan, C.; Guo, Y.; Zuo, Z.; Roskilly, A.P.; Jia, B. Research on combustion process of a free piston diesel linear generator. *Appl. Energy* **2016**, *161*, 395–403. [CrossRef]
7. Feng, H.; Guo, C.; Jia, B.; Zuo, Z.; Guo, Y.; Roskilly, T. Research on the intermediate process of a free-piston linear generator from cold start-up to stable operation: Numerical model and experimental results. *Energy Convers. Manag.* **2016**, *122*, 153–164. [CrossRef]
8. Jia, B.; Mikalsen, R.; Smallbone, A.; Zuo, Z.; Feng, H.; Roskilly, A.P. Piston motion control of a free-piston engine generator: A new approach using cascade control. *Appl. Energy* **2016**, *179*, 1166–1175. [CrossRef]
9. Mikalsen, R.; Roskilly, A.P. A review of free-piston engine history and applications. *Appl. Therm. Eng.* **2007**, *27*, 2339–2352. [CrossRef]
10. Max, E. Fpec, free piston energy converter. In Proceedings of the 21st Electric Vehicle Symposium & Exhibition (EVS), Monaco, April 2005.
11. Jia, B.; Smallbone, A.; Mikalsen, R.; Feng, H.; Zuo, Z.; Roskilly, A.P. Disturbance analysis of a free-piston engine generator using a validated fast-response numerical model. *Appl. Energy* **2017**, *185*, 440–451. [CrossRef]
12. Mikalsen, R.; Roskilly, A.P. The design and simulation of a two-stroke free-piston compression ignition engine for electrical power generation. *Appl. Therm. Eng.* **2008**, *28*, 589–600. [CrossRef]
13. Jia, B.; Zuo, Z.; Tian, G.; Feng, H.; Roskilly, A.P. Development and validation of a free-piston engine generator numerical model. *Energy Convers. Manag.* **2015**, *91*, 333–341. [CrossRef]
14. Jia, B.; Smallbone, A.; Zuo, Z.; Feng, H.; Roskilly, A.P. Design and simulation of a two-or four-stroke free-piston engine generator for range extender applications. *Energy Convers. Manag.* **2016**, *111*, 289–298. [CrossRef]
15. Goldsborough, S.S.; Blarigan, P.V. *A Numerical Study of a Free Piston IC Engine Operating on Homogeneous Charge Compression Ignition Combustion*; SAE Technical Paper; SAE International: Warrendale, PA, USA, 1999.
16. Li, Q.; Xiao, J.; Huang, Z. Simulation of a two-stroke free-piston engine for electrical power generation. *Energy Fuels* **2008**, *22*, 3443–3449. [CrossRef]
17. Atkinson, C.M.; Petreanu, S.; Clark, N.; Atkinson, R.J.; McDaniel, T.I.; Nandkumar, S.; Famouri, P. *Numerical Simulation of a Two-Stroke Linear Engine-Alternator Combination*; SAE Technical Paper; SAE International: Warrendale, PA, USA, 1999.
18. Shoukry, E.; Taylor, S.; Clark, N.; Famouri, P. *Numerical Simulation for Parametric Study of a Two-Stroke Direct Injection Linear Engine*; SAE Technical Paper; SAE International: Warrendale, PA, USA, 2002.
19. Clark, N.; McDaniel, T.; Atkinson, R.; Nandkumar, S.; Atkinson, C.; Petreanu, S.; Tennant, C.; Famouri, P. Modeling and development of a linear engine. In Proceedings of the Spring Technical Conference of the ASME Internal Combustion Engine Division, Fort Lauderdale, FL, USA, 26 April 1998; pp. 26–29.
20. Clark, N.; Nandkumar, S.; Famouri, P. *Fundamental Analysis of a Linear Two-Cylinder Internal Combustion Engine*; SAE Technical Paper; SAE International: Warrendale, PA, USA, 1998.
21. Shoukry, E.F. *Numerical Simulation for Parametric Study of a Two-Stroke Compression Ignition Direct Injection Linear Engine*; West Virginia University: Morgantown, WV, USA, 2003.
22. Nandkumar, S. *Two-Stroke Linear Engine*; West Virginia University: Morgantown, WV, USA, 1998.
23. Mikalsen, R.; Roskilly, A.P. Performance simulation of a spark ignited free-piston engine generator. *Appl. Therm. Eng.* **2008**, *28*, 1726–1733. [CrossRef]
24. Blarigan, P.V.; Paradiso, N.; Goldsborough, S. *Homogeneous Charge Compression Ignition with a Free Piston: A New Approach to Ideal Otto Cycle Performance*; SAE Technical Paper; SAE International: Warrendale, PA, USA, 1998.

25. Goldsborough, S.S.; Blarigan, P.V. *Optimizing the Scavenging System for a Two-Stroke Cycle, Free Piston Engine for High Efficiency and Low Emissions: A Computational Approach*; SAE Technical Paper; SAE International: Warrendale, PA, USA, 2003.
26. Goldsborough, S.S. *A Numerical Investigation of a Two-Stroke Cycle, Hydrogen-Fueled, Free Piston Internal Combustion Engine*; Colorado State University: Fort Collins, CO, USA, 1998.
27. Mao, J.; Zuo, Z.; Feng, H. Parameters coupling designation of diesel free-piston linear alternator. *Appl. Energy* **2011**, *88*, 4577–4589. [CrossRef]
28. Mao, J.; Zuo, Z.; Li, W.; Feng, H. Multi-dimensional scavenging analysis of a free-piston linear alternator based on numerical simulation. *Appl. Energy* **2011**, *88*, 1140–1152. [CrossRef]
29. Lim, O.; Hung, N.B.; Oh, S.; Kim, G.; Song, H.; Iida, N. A study of operating parameters on the linear spark ignition engine. *Appl. Energy* **2015**, *160*, 746–760. [CrossRef]
30. Jia, B.; Zuo, Z.; Feng, H.; Tian, G.; Roskilly, A.P. *Development Approach of a Spark-Ignited Free-Piston Engine Generator*; SAE Technical Paper; SAE International: Warrendale, PA, USA, 2014.
31. Jia, B.; Tian, G.; Feng, H.; Zuo, Z.; Roskilly, A.P. An experimental investigation into the starting process of free-piston engine generator. *Appl. Energy* **2015**, *157*, 798–804. [CrossRef]
32. Miao, Y.; Zuo, Z.; Feng, H.; Guo, C.; Song, Y.; Jia, B.; Guo, Y. Research on the combustion characteristics of a free-piston gasoline engine linear generator during the stable generating process. *Energies* **2016**, *9*, 655. [CrossRef]
33. Hansson, J. Analysis and Control of a Hybrid Vehicle Powered by Free-Piston Energy Converter. Ph.D. Thesis, Royal Institute of Technology, Stockholm, Sweden, 2006.
34. Jia, B.; Smallbone, A.; Feng, H.; Tian, G.; Zuo, Z.; Roskilly, A.P. A fast response free-piston engine generator numerical model for control applications. *Appl. Energy* **2016**, *162*, 321–329. [CrossRef]
35. Harris, C.M.; Piersol, A.G.; Paez, T.L. *Harris' Shock and Vibration Handbook*; McGraw-Hill: New York, NY, USA, 2002.